IBRACON Structures and Materials Journal
Revista IBRACON de Estruturas e Materiais
ISSN 1983-4195 ismj.org

ORIGINAL ARTICLE

Numerical analysis of the influence of reinforcement ratio on the behavior of on-top laterally loaded concrete piles

Análise numérica da influência da taxa de armadura no comportamento de estacas de concreto carregadas horizontalmente no topo

Leonardo Bonfante Greco[a]
Jeselay Hemetério Cordeiro dos Reis[a]
Rafael Alves de Souza[a]

[a]Universidade Estadual de Maringá - UEM, Programa de Pós-graduação em Engenharia Civil, Maringá, PR, Brasil

Received 02 August 2023
Revised 29 April 2024
Accepted 29 April 2024

Abstract: In this research, the behavior of laterally loaded piles is studied, wherein flexure-induced tensile stresses are responsible for the cracking process. The primary focus lies on investigating the direct influence of the reinforcement ratio on the pile's behavior. Through a comprehensive numerical 3D finite element analysis (FEM), the effects of varying reinforcement ratios on laterally loaded piles are examined in terms of displacements, stresses, and yielding. Employing the ABAQUS software, distinct constitutive models are used for concrete piles (Concrete Damage Plasticity model), soil (Mohr-Coulomb model), and steel rebars (elasto-plastic model). The results reveal that higher reinforcement ratios lead to reduced cracking propagation and lateral displacement, consequently enhancing the lateral capacity of concrete piles within the limitations of the soil bearing capacity. Moreover, it is observed that the depth at which a plastic hinge forms in longer piles shows minimal sensitivity to changes in the reinforcement ratio. Additionally, the increase in reinforcement ratio is found to result in decreased bending moments on the piles, accompanied by reduced strains and stresses in the surrounding soil. Overall, this investigation provides crucial insights into optimizing pile design by considering the reinforcement ratio, ultimately enhancing the structural performance and integrity of laterally loaded piles.

Keywords: cracking; laterally loaded piles; reinforcement ratio; numerical analysis; finite element method.

Resumo: Esta pesquisa aborda o comportamento de estacas carregadas lateralmente, onde as tensões de tração induzidas pela flexão são responsáveis pelo processo de fissuração. O foco principal reside em investigar a influência direta da taxa de armadura no comportamento das estacas. Por meio de uma análise numérica de elementos finitos em 3D (MEF), são examinados os efeitos de diferentes taxas de armadura em estacas carregadas lateralmente, considerando deslocamentos, tensões e deformações. Utilizando o software ABAQUS, modelos constitutivos distintos são aplicados para estacas de concreto (Concrete Damage Plasticity), solo (Mohr-Coulomb) e barras de aço (modelo elastoplástico). Os resultados revelam que maiores taxas de armadura levam a uma redução na propagação de fissuras e no deslocamento lateral, consequentemente, aumentando a capacidade lateral das estacas de concreto dentro das limitações da capacidade de carga do solo. Além disso, observa-se que a profundidade em que se desenvolve uma rótula plástica em estacas longas é pouco suscetível a mudanças na taxa de armadura. Adicionalmente, o aumento na taxa de armadura resulta em menor momento fletor nas estacas, acompanhado de redução nas deformações e tensões no solo adjacente. De modo geral, esta investigação oferece informações cruciais para otimizar o projeto de estacas, considerando a taxa de armadura, melhorando a performance estrutural e a integridade das estacas carregadas lateralmente.

Palavras-chave: fissuração, estacas carregadas lateralmente, taxa de armadura, análise numérica, método dos elementos finitos.

How to cite: L. B. Greco, J. H. C. Reis, and R. A. Souza, "Numerical analysis of the influence of reinforcement ratio on the behavior of on-top laterally loaded concrete piles," *Rev. IBRACON Estrut. Mater.*, vol. 17, no. 4, e17413, 2024, https://doi.org/10.1590/S1983-41952024000400013.

Corresponding author: Leonardo Bonfante Greco. E-mail: leogreco95@gmail.com
Financial support: This study was financed in part by the Coordenação de Aperfeiçoamento de Pessoal de Nível Superior - Brasil (CAPES) - Finance Code 001.
Conflict of interest: Nothing to declare.
Data Availability: The data that support the findings of this study are available from the corresponding author, LBG, upon reasonable request.

1 INTRODUCTION

Pile foundations are widely used in modern engineering, when the first layers of soil do not exhibit the necessary load capacity for shallow foundations. Although piles are very efficient in transferring vertical loads to the soil mass while suffering minor displacement, they are often subjected to horizontal loads such as wind force, earthquakes, wave impact, traffic, etc. The design of laterally loaded piles is a common and complex problem of soil-structure interaction, and its bearing capacity can be either governed by the pile as a structural element or by the soil capacity [1]–[3].

Poulos and Davis [1] observed that piles behave in two different ways regarding the relation between the pile and the soil stiffness parameters and classified them as *short* and *long* piles. A laterally loaded *short* pile would rotate as a whole such as a rigid body, while *long* piles would present a flexible behavior, such as a cantilever beam, and develop a plastic hinge at a given depth [4].

Since *long* piles are generally used more often than *short* piles for general structures such as buildings, the present paper focuses on studying this specific behavior. A similar work regarding *short* piles can be found in Conte et al. [5].

Several authors [1], [4], [6]–[11] proposed analytical solutions to assess the pile lateral capacity and the stress distribution in the soil. Based on these solutions and in addition to Winkler's model for beams over an elastic surface, it is possible to represent the problem in diverse scenarios, such as the different soil layers and pile's response to a given reduction in the cross-section inertia. However, these solutions cannot account for the soil continuity and soil-structure interaction, nor assess the concrete cracking patterns and the effects of the reinforcement ratio on the pile's behavior.

The Finite Element Method (FEM) offers the possibility to model the soil as a continuum element and to apply constitutive models to the soil and the pile considering the soil plasticity, the concrete damage, the rebar yielding, and it has been widely used for such [12]–[16]. Hence, it is possible to consider a wider range of variables that may interfere on the soil-structure behavior, even with basic experimental data as input [4], [5].

Martins et al. [16], Conte et al. [5], Qinglai and Yufeng [2] and Venkateswarlu and Hemanth [17] studied the effects of the reinforcement ratio on the behavior of beams and piles. The studies pointed that the reinforcement ratio exhibit influence on cracking propagation. For lower ratios, greater cracking patterns were observed, resulting in greater stresses and strains on rebar and concrete. Moreover, the authors also observed that the rupture method is also different based on the reinforcement ratio of the pile: for piles with lower ratios, the load capacity is governed by the pile, while for higher reinforcement ratios, the soil capacity is responsible for limiting the group load capacity.

Alonso [18] affirms that the failure in on-top laterally loaded long piles is given due to the emergence of one or two plastic hinges. Therefore, it was hypothesized that the reinforcement ratio and the rebar distribution could exert influence on the depth which the plastic hinges are formed in each case.

This study aims to enlighten the behavior of flexible laterally loaded reinforced concrete piles for different reinforcement ratios. To achieve this objective, a 3D finite element model was developed using the software ABAQUS. The nonlinear behavior of the soil, the concrete cracking and the rebar yielding were accounted for by applying the suitable constitutive models for each element. The developed model was validated by comparison with the field test results from Abreu [19].

2 FINITE ELEMENT MODELING

2.1 Model geometry and mesh definition

The finite element model developed in this study is based on the experimental data from Abreu [19]. The material properties for concrete and the pile geometry are the same, while the soil properties and the dimensions for the soil mass were adjusted to obtain similar results, as discussed further ahead in this article. Table 1 shows the geometric properties of the pile.

Table 1. Geometric parameters for the pile from Abreu [19]

Diameter *D* (cm)	Total Length (m)	Bored Length (m)	Rebar	Reinforcement Ratio
30	8.00	7.50	4 Ø 16mm	1.14%

The soil mass was modeled as a cylindrical body following the recommendations from Dong et al. [20] to avoid boundary effects. Then, the dimensions were adjusted based on a sensibility analysis aiming for satisfactory results while minimizing the computational cost as much as possible. The cylindrical model representing the soil was then

defined with a diameter of 20D and a length of 30D, with a 5D gap between the pile tip and the bottom of the cylindrical body, where D is the diameter of the pile. The general model geometry is shown in Figure 1a.

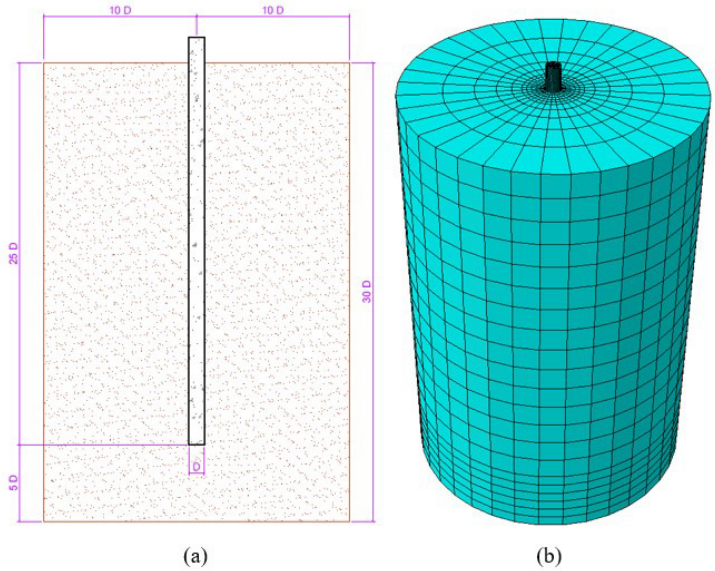

Figure 1. General finite element model (a) geometry in cut; (b) mesh distribution

The same finite element was used to constitute soil and pile: the C3D8R element, an 8-node hexahedron with linear interpolation and reduced integration. The C3D8R element general formulation is described in Equation 1.

$$u = \frac{1}{8}(1-g)(1-h)(1-r)u_1 + \frac{1}{8}(1+g)(1-h)(1-r)u_2 + \frac{1}{8}(1+g)(1+h)(1-r)u_3 + \frac{1}{8}(1-g)(1+h)(1-r)u_4 + \frac{1}{8}(1-g)(1-h)(1+r)u_5 + \frac{1}{8}(1+g)(1-h)(1+r)u_6 + \frac{1}{8}(1+g)(1+h)(1+r)u_7 + \frac{1}{8}(1-g)(1+h)(1+r)u_8 \quad (1)$$

The steel rebars were modeled using the T3D2 element, a 2-node truss element with linear formulation (Equation 2).

$$u(g) = \frac{1}{2}(1-g)u_1 + \frac{1}{2}(1+g)u_2 \quad (2)$$

The finite element mesh was defined through a sensibility analysis considering the relation between the result's accuracy and the computational cost for each variation tested. A 4D diameter region with a refined mesh was created around the pile, and a bias pattern was used for the outer mesh. Figure 1b shows the meshed numerical model while Table 2 shows a summary of the mesh size and element type used for each region.

Table 2. Mesh Summary

Region	Element Type	Mesh Size
Refined mesh (soil)	C3D8R	D/3
Bias mesh (soil)	C3D8R	2D/3 to 4D/3
Vertical mesh (soil)	C3D8R	4D/3
Pile	C3D8R	D/10
Rebar	T3D2	D/10

2.2 Rheological models and material properties

As this article presents a numerical model to assess a pile's lateral capacity under different reinforcement conditions based on the experimental tests results shown in Abreu [19], it is natural to consider for the numerical analysis the same soil profile where the experiments were conducted (Figure 2).

The reliability of a finite element model relies on the rheological models applied for the materials, they need to represent the reality of the problem in study, whatever it is. More complex constitutive models require complex and not often available data for input. Considering the need to apply a model that could represent the elasto-plastic behavior of the soil while requiring basic input data such as the friction angle, the cohesion and dilatancy angle, which are basic design parameters used in engineering practice, the Mohr-Coulomb criteria would be the best option. As this model has been widely and successfully used in geotechnical research, it was assigned to represent the soil behavior in the present study.

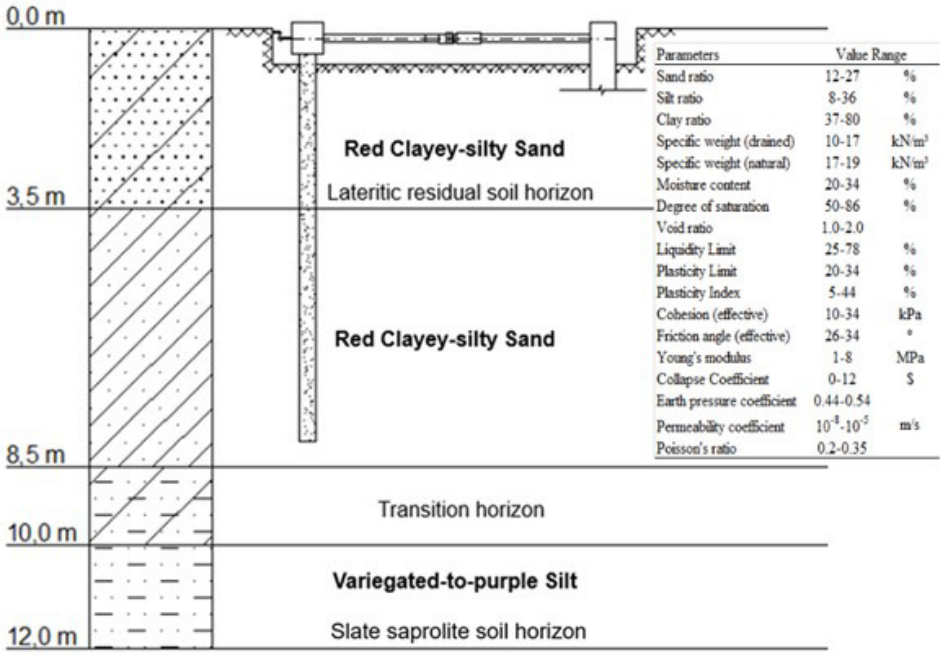

Figure 2. Characteristic soil profile at UnB's experimental site, adapted from Abreu [19]

As shown in Figure 2, the whole pile body is contained within a Red Clayey-Silty Sand. Thus, in order to reduce the number of variables in the model along with the computational cost, the authors chose to model the soil mass as a uniform body, with the same material parameters from top to bottom. At first, the soil parameters applied to the numerical model were the same used in Abreu's [19] analysis but were adjusted by the authors of this research in the validation phase, until the numerical model's results were close enough to the experimental results.

The Concrete Damage Plasticity (CDP) was established to represent the concrete behavior, an ABAQUS's signature model that correlates the stress-strain relationships (Figure 3) from the input data to simulate concrete cracking and crushing. Such model has been proven to satisfactorily represent concrete damage [5], [12] –[16].

The Figure 3 describes the relationship between inelastic strain, plastic strain, compression stress and strain of concrete. The damage parameter d_c, plastic strain ε_c^{pl}, and inelastic strain ε_c^{in} were determined using the formulations from Hordjik [21]. The plastic behavior of concrete parameters such as dilation angle (ψ), the plastic potential eccentricity of concrete (ϵ), the ratio of compressive stress in the biaxial state to the compressive stress in the uniaxial state (σ_{b0}/σ_{c0}), the shape factor of the yielding surface in the deviatoric plane (K_c) and viscosity parameter were determined by calibration.

A more detailed approach on the properties and sensibility of the variables in the CDP model can be found in Earij et al. [14].

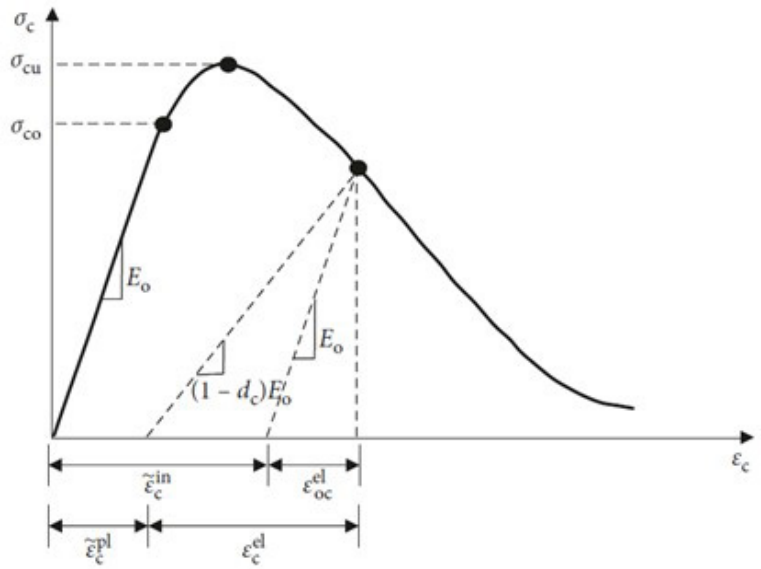

Figure 3. The plain concrete damage plasticity model

The steel rebars were modeled using the standard elasto-plastic behavior, where the rebars would present a linear-elastic behavior when submitted to a stress lower than the yielding stress *fyk*. Then, for stresses greater than *fyk*, the rebars would present plastic strains until reaching the established limit of 1%. The specific parameters used in this study can be found in Table 3.

Table 3. Material parameters for the finite element model

Soil Parameters							
E_s (MPa)	c' (kPa)	φ' (º)		γ_n (kN/m^3)		v	
15	10	25		16		0.3	
Concrete Parameters							
f_{ck} (MPa)	E_c (GPa)	v	ψ (º)	ϵ	f_{b0}/f_{c0}	K	Viscosity
20	20	0.2	25	0.1	1.16	0.667	0.01
Steel Rebar Parameters							
f_{yk} (MPa)		E_y (GPa)				v	
500		210				0.3	

Where E_s, E_c and E_y are the Young's Modulus for the soil, concrete and steel rebars, respectively; c' is the drained cohesion of the soil; φ' is the drained friction angle for the soil; γ_n is the specific weight for the soil; v is the Poisson's ratio for each material; f_{ck} is the characteristic compressive strength for the concrete; f_{yk} is the characteristic yield strength for the steel; ψ, ϵ, f_{b0}/f_{c0}, K and Viscosity are the CDP general parameters.

The surface contact in ABAQUS is modeled using the Normal and Tangential behavior parameters. For Normal behavior, the Hard Contact model was assigned, with linear penalization. This model allows the interpenetration of the elements in contact to facilitate convergence, while not compromising the results. The Tangential behavior was defined using the Coulomb criteria, governed by the Equation 3:

$$\tau_{crit} = \mu \cdot p \tag{3}$$

Where τ_{crit} is the critical shear stress in the surface; μ is the friction coefficient; and p is the force acting in the surface.

The slip between the two surfaces in contact will happen when the equivalent shear stress in the surface τ_{eq} reaches the value of τ_{crit}. The assigned value of μ for the model was 0.34, calculated based on the friction correlations in literature between soil and concrete, and tested in the sensibility analysis.

2.3 Parametric study

Table 4. Summary of Models for different values of ρ

Model	Rebar Arrangement	Reinforcement Ratio ρ (%)	Applied Lateral Loading (kN)
1	4 Ø 10mm	0.44	34
2	6 Ø 12.5mm	1.04	34
3	8 Ø 16mm	2.28	34
4	6 Ø 12.5mm	1.04	57
5	8 Ø 16mm	2.28	70

In order to investigate the effects of variation of the reinforcement ratio on the behavior of laterally loaded piles, analyzing cracking propagation, displacements, stresses and strains, 5 situations were elaborated for the study (Table 4).

Figure 4 shows the cross-sectional profile for each model.

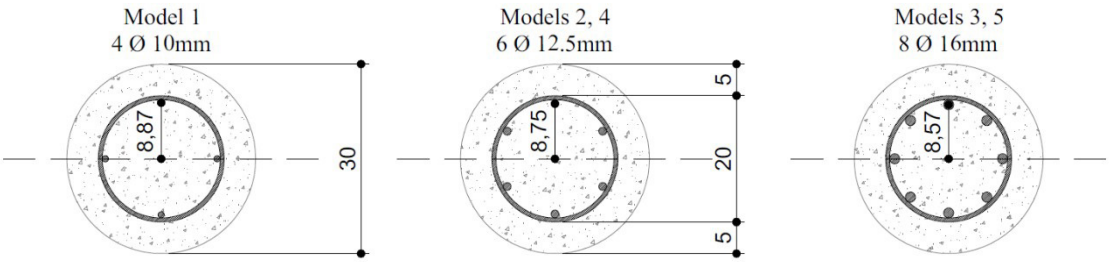

Figure 4. Cross-section view for each pile model (units in cm)

The configuration for Model 1 with 4 steel bars was chosen based on the combination of requirements from the Brazilian Standards NBR 6118 [22] and NBR 6122 [23] along with practical experience and curiosity. The former defines that the diameter for steel bars in concrete columns and piles must be equal to or greater than 10 millimeters and a minimum number of 6 bars, while the latter states that a pile under pure compression loading below a defined limit could be reinforced with a minimum reinforcement ratio of 0.4%.

Naturally, the minimum reinforcement ratio defined by [23] can't be applied for flexed piles, but as this condition is widely used in practice the authors decided to bring it to the test. Thus, the configurations for Models 2 and 3 were defined by doubling the reinforcement ratio of the previous model.

The pile type and rebar length for the piles in this study were the same as adopted in [19]. It is a CHD (Continuous Helical Displacement) pile and the rebars were 3 meters long.

3 RESULTS AND DISCUSSION

3.1 Model validation

In Abreu's [19] experimental case, a CHD pile reinforced with 4 steel bars of 16.00 mm diameter reached failure under a 34 kN lateral loading. In order to validate the numerical model by comparison with the field test results, the exact same situation was modeled in ABAQUS. The material parameters presented earlier were defined during the calibration phase, aiming for the most accurate possible result, and the load application steps where the numerical results were measured are controlled by the software, while the authors limited the load increment between each step in a maximum of 5% the total loading. The comparison between the measured and calculated Lateral Load *versus* Lateral Displacement curves are shown in Figure 5. The resulting R^2 coefficient between curves is 0.9982.

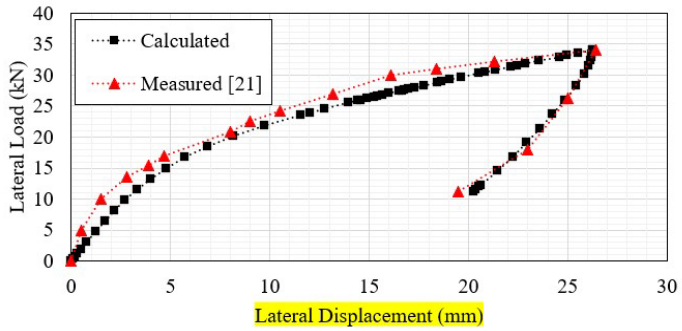

Figure 5. Comparison between measured and calculated Load versus Displacement curves

The curves in Figure 5 show that failure occurred at a displacement of, approximately, 26 mm for a 34 kN loading. The displacement value is roughly less than 10% the pile's diameter, which is usually assumed to be the pile limiting acceptable displacement in design and testing practice.

3.2 Variation of the reinforcement ratio

Five models were elaborated to study the maximum displacements, stresses, and strains in steel and concrete and the cracking propagation under horizontal loading for different reinforcement ratios, as summarized in Table 4.

An unloading phase was also added to each case, aiming to evaluate displacement recovery. The load *versus* displacement curves for each model is shown in Figure 6.

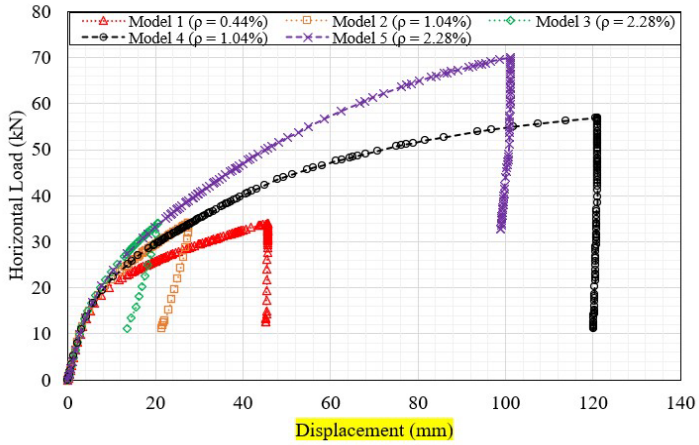

Figure 6. Load versus displacement curves for different values of ρ

Analyzing curves from Models 1-3, with different values of ρ for the same applied load, it shows that the maximum displacement values decrease with the increase of ρ. Moreover, the displacement recovery for Model 1 is negligible, evidence of structural failure, while Models 2 and 3 presented a displacement recovery of 22% and 33%, respectively. Then, the structural failure for the same values of ρ at Models 2 and 3 can be observed for greater loadings, as shown by the curves from Models 4 and 5. The stresses, strains, the maximum bending moments, and the position of the neutral axis at the moment of the structural failure are available at Table 5.

Table 5. Strains and stresses at failure

Model	ε_c	ε_y	σ_c (MPa)	σ_y (MPa)	M (kN.m)	Neutral Axis Pos. (mm)
1	0.2440%	1.0360%	24.86	500.00	65.90	45.50
4	0.3883%	0.8225%	27.11	500.00	71.86	69.13
5	0.3569%	0.6946%	27.06	500.00	71.73	75.74

Where ε_c and ε_y are the strains for concrete and steel, respectively; σ_c and σ_y are the stresses for concrete and steel, respectively; M is the bending moment; and the position of the neutral axis is measured from the compressed surface towards the opposite surface of the pile.

For the present study, the strain limit for concrete and steel are taken as 0,35% and 1%, respectively, as stated by the Brazilian design standard NBR 6118 [22]. Then, Table 5 shows that the failure of the pile occurred by yielding of the steel rebar for Model 1, while it is caused by concrete crushing for Models 4 and 5.

The position of the neutral axis gets closer to the center of the pile for increasing values of ρ, even at failure, which indicates a better preservation of the cross-section of the pile by reducing cracking propagation. This is better illustrated at Figure 7, which shows the cracking patterns for Models 1-3.

There is also a slight increase (~10%) in the maximum bending moment and compressive stress at failure when comparing Model 1 with Model 4 or 5, but there's no considerable difference between Models 4 and 5. This indicates that, even with increasing values for the reinforcement ratio, the maximum bending moment resisted by the pile will not change considerably. Yet, when comparing Models 1-3, with the same applied loading but increasing values of ρ, the reduction of cracking and the consequent preservation of the cross-sectional inertia will result in lesser values for the maximum observed bending moments (Figure 8).

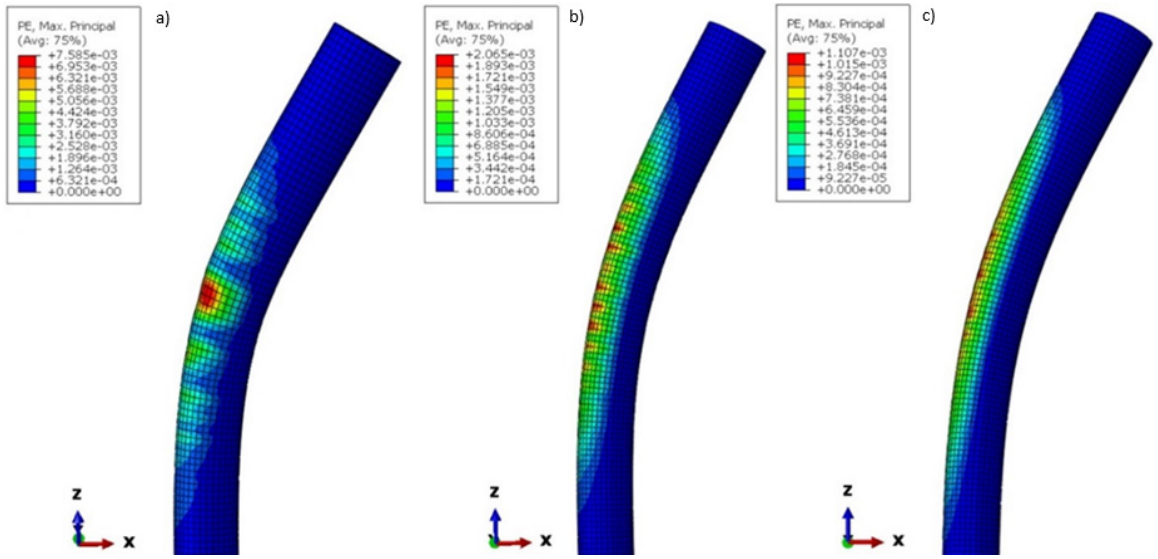

Figure 7. Cracking patterns for models (a) 1; (b) 2; (c) 3

Where *PE, Max. Principal* is the maximum plastic strain observed for each element.

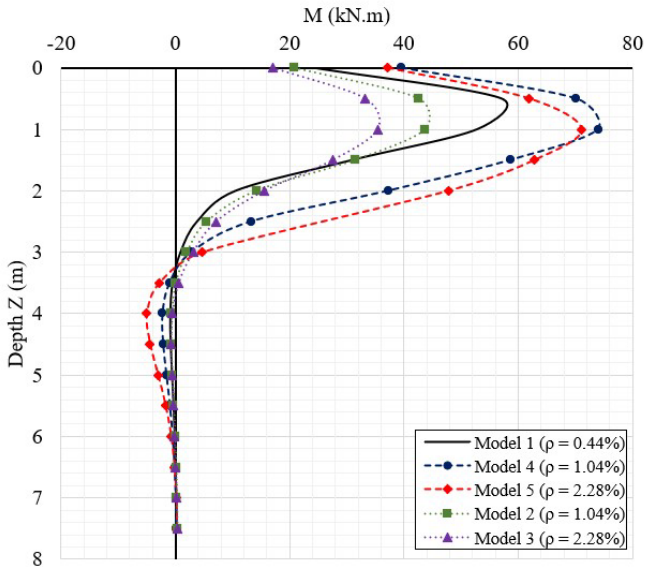

Figure 8. Bending moment versus depth curves

The increase of the reinforcement ratio doesn't increase, significantly, the cross-sectional inertia, but it results in a stiffer behavior by the preservation of the cross-sectional inertia due to reduced cracking, as shown by the Moment *versus* curvature curves for Models 1, 4 and 5 in Figure 9.

The maximum tensile stresses and strains in the steel rebars for Models 1-3 are presented in Figure 10 and Figure 11, respectively. There's a notable reduction in the tensile stresses with the increase of the reinforcement ratio. However, this reduction cannot be attributed exclusively to the effects of the cracking reduction, as it is natural to have a lower stress value with the increase of the available steel area.

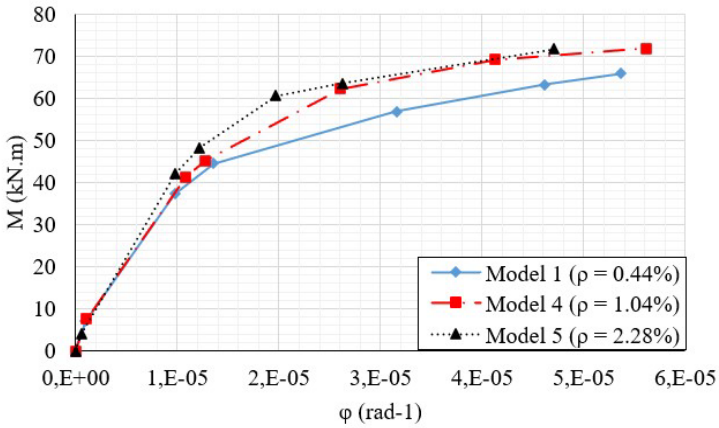

Figure 9. Moment versus curvature diagram for Models 1, 4 and 5.

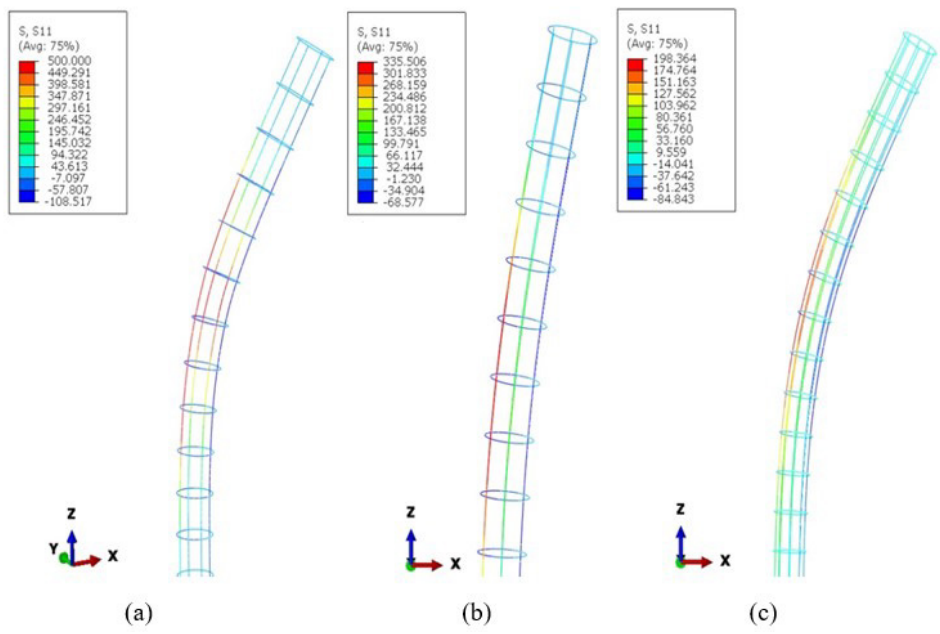

Figure 10. Tensile stresses (MPa) in rebar for Models (a) 1; (b) 2; (c) 3

The results show that the reinforcement ratio has major influence on the behavior of a pile, as observed in the literature [2], [5]. The increase for the values of ρ is responsible for the stiffer behavior of the pile due to reduced cracking and consequent preservation of the cross-sectional inertia. However, analyzing the differences in the behavior between the models, it is seen that the effectiveness of increasing the reinforcement ratio has diminishing returns, which means that there's an optimal reinforcement ratio that offers a satisfactory behavior with reduced cost.

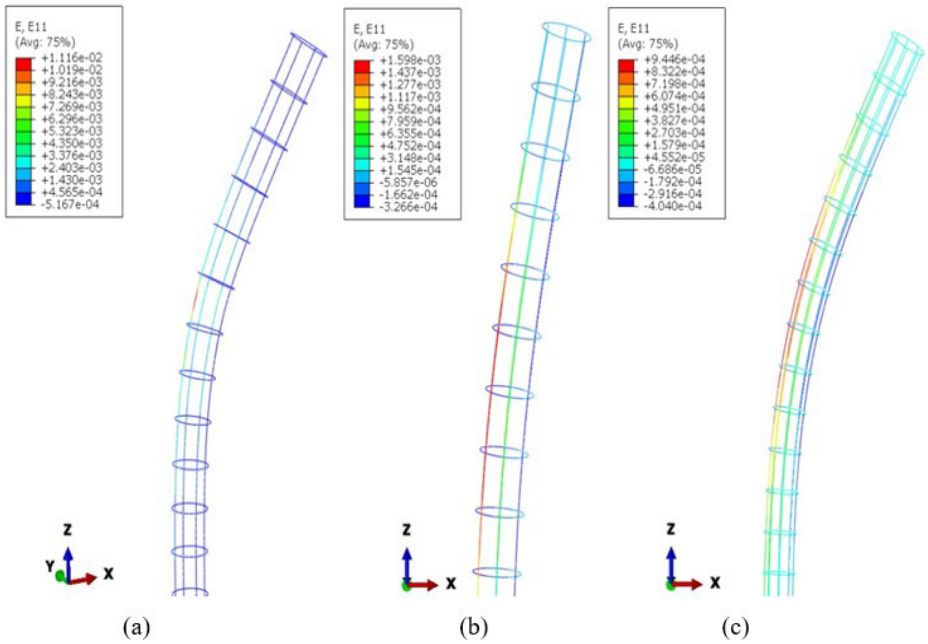

Figure 11. Strains in steel rebar for Models (a) 1; (b) 2; (c) 3

An additional analysis was conducted in order to observe the effects of rebar distribution on a pile's lateral behavior. With this objective, 9 numerical models were developed, with piles reinforced by 4, 6 and 8 steel bars of 10.00 mm, 12.50 mm and 16.00 mm under a 34 kN lateral loading. The variable response for this analysis was the lateral displacement at the top of the pile, and the results are shown in Figure 12.

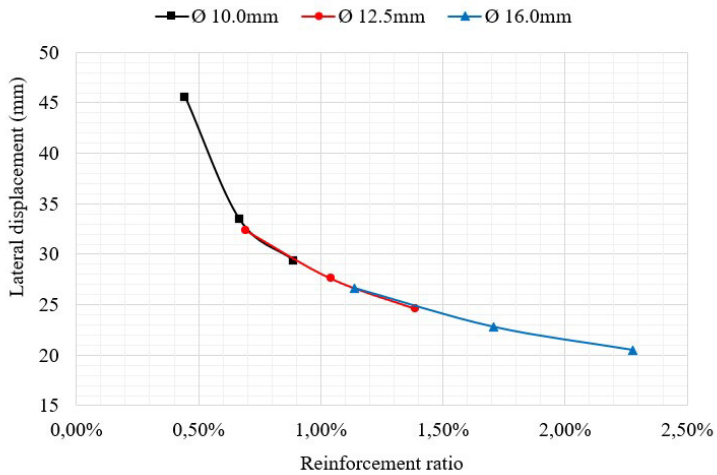

Figure 12. Lateral displacement versus Reinforcement ratio curves for different reinforcement configurations

Analyzing the test results shown in Figure 12 it is noticeable that while the reinforcement ratio exerted influence on the pile's lateral response, different rebar distributions for the same reinforcement ratio exhibited very similar results.

4 CONCLUSIONS

A 3D finite element approach was conducted to evaluate the effects of reinforcement ratio on laterally loaded piles. Based on the obtained results formerly discussed it is possible to conclude that:

(a) The increase in the reinforcement ratio on piles was proven responsible for reducing cracking propagation, and consequently preserving the cross-sectional inertia and inducing a stiffer behavior from the laterally loaded pile, presenting lesser values for displacements, moments, stresses, and strains.

(b) Despite that a greater reinforcement ratio can reduce the displacements and bending moments developed along the pile depth, the maximum bending moment that a certain cross-section can resist doesn't seem to change significantly with it, although a greater loading would be necessary to induce such moment.
(c) The design of laterally loaded piles must consider the influence of the reinforcement ratio on the behavior of the pile, as a different value of ρ could increase or decrease important design parameters.
(d) The rebar distribution under the same reinforcement ratio showed negligible influence on the pile's lateral response.
(e) The ABAQUS's Concrete Damage Plasticity (CDP) model presented good simulation performance, as also stated by previous literature.

REFERENCES

[1] H. G. Poulos and E. H. Davis *Pile Foundation Analysis and Design*, 1st ed., Malabar, FL, USA: Krieger Pub. Company Inc., 1980.

[2] F. Qinglai and G. Yufeng, "Effect of reinforcement ratio and vertical load level on lateral capacity of bridge pile foundations," *Pol. Marit. Res.*, vol. 25, no. S3, pp. 120–126, Jan 2018.

[3] A. M. Ebid, "Simplified approach to consider cracking effect on the behavior of laterally loaded RC piles," *Int. J. Innov. Res. Sci., Eng. and Tech.*, vol. 77, no. 10, Oct., 2015.

[4] K. Fleming, A. Weltman, M. Randolph, and K. Elson, *Piling Engineering*, 3rd ed., New York, NY, USA: Taylor & Francis, 2009.

[5] E. Conte, A. Troncone, and M. Vena, "Nonlinear three-dimensional analysis of reinforced concrete piles subjected to horizontal loading," *Comput. Geotech.*, vol. 49, pp. 123–133, Apr 2013.

[6] B. B. Broms, "Lateral resistance of piles in cohesive soils," *J. Soil Mech. Found. Div.*, vol. 90, no. 2, pp. 27–63, Mar 1964.

[7] B. B. Broms, "Lateral resistance of piles in cohesionless soils," *J. Soil Mech. Found. Div.*, vol. 90, no. 3, pp. 123–156, May 1964.

[8] H. Matlock and L. C. Reese, "Generalized solutions for laterally loaded piles," *J. Soil Mech. Found. Div.*, vol. 86, no. 5, Oct 1960.

[9] J. Brinch Hansen, "The ultimate resistance of rigid piles against transversal forces," *Danish Geotech. Inst. Bulletin*, no. 12, pp. 5-9, 1961.

[10] L. Zhang, F. Silva, and R. Grismala, "Ultimate lateral resistance to piles in cohesionless soils," *J. Geotech. Geoenviron. Eng.*, vol. 131, no. 1, pp. 78–83, Jan 2005.

[11] L. C. Reese and W. Van Impe *Single Piles and Pile Groups Under Lateral Loading*, 2nd ed., London, UK: CRC Press, 2011.

[12] M. Pazdan, "FEM modelling of the static behaviour of reinforced concrete beams considering the nonlinear behaviour of the concrete," *Stud. Geotech. Mech.*, vol. 43, no. 3, pp. 206–223, Apr 2021.

[13] A. Yazir, M. K Effendi, A. Taveriyanto, and H. Apriyatno, "Analysis of strengths of reinforced concrete beam structures with cfrp sheet using ABAQUS Software 6.14," *Jurnal Teknik Sipil & Per.*, vol. 21, no. 1, Jan., 2019.

[14] A. Earij, G. Alfano, K. Cashell, and X. Zhou, "Nonlinear three–dimensional finite–element modelling of reinforced–concrete beams: computational challenges and experimental validation," *Eng. Fail. Anal.*, vol. 8, pp. 92–115, Dec 2017.

[15] K. N. Gowda, S. A. K. Zai, J. Chethankumar, and K. N. Aswini Kumar, "Finite element analysis of flexural behaviour recycled aggregate concrete beam using ABAQUS," *Int. J. Curr. Res.*, vol. 13, pp. 18727–18732, Sep 2021.

[16] P. A. Martins, P. R. L. Lima, J. M. Lima, and G. J. B. Santos, "Análise numérica de vigas de concreto armado com diferentes taxas de armadura usando modelo de plasticidade," *J. Res. Innov. Civil Eng.*, vol. 1, no. 1, Jun., 2021.

[17] B. Venkateswarlu, and K. S. Hemanth, "Flexural behavior of reinforced concrete beam by finite element method," *Int. J Eng. Sci. Comp.*, vol. 8, no. 6, Jun., 2018.

[18] U. R. Alonso, *Dimensionamento de Fundações Profundas.* 2 ed., São Paulo, Brazil: Blucher, 2012.

[19] J. A. Abreu, "Avaliação do comportamento de grupos de fundação carregados lateralmente em solo poroso colapsível e tropical do Distrito Federal," Dissertation, Fac. de Tec., Univ. de Brasília, Brasília, DF, 2014.

[20] J. Dong, F. Chen, M. Zhou, and X. Zhou, "Numerical analysis of the boundary effect in model tests for single pile under lateral load," *Bull. Eng. Geol. Environ.*, vol. 77, pp. 1057–1068, Aug 2018.

[21] D. A. Hordjik, "Local approach to fatigue of concrete," Thesis, Technische Universiteit Delft, Delft, 1991.

[22] Associação Brasileira de Normas Técnicas, *Design of Concrete Structures,* NBR 6118, 2023. (In portuguese).

[23] Associação Brasileira de Normas Técnicas, *Design and Construction of Foundations*, NBR 6122, 2019. (In portuguese).

Author contributions: LBG: conceptualization, methodology, data curation, writing; JHCR: conceptualization, supervision, methodology, formal analysis; RAS: formal analysis.

Editors: Osvaldo Manzoli, Daniel Carlos Taissum Cardoso.